



Study of *p*-(3-carboxy-1-adamantyl)-calix[4]arene with hydrogen bonds along the upper and lower rim by IR spectroscopy and DFT

V. L. Furer¹ · L. I. Potapova¹ · D. V. Chachkov² · I. M. Vatsouro³ · V. V. Kovalev³ · E. A. Shokova³ · V. I. Kovalenko⁴

Received: 31 March 2020 / Accepted: 10 June 2020
© Springer-Verlag GmbH Germany, part of Springer Nature 2020

Abstract

The IR spectra of *p*-(3-carboxy-1-adamantyl)-calix[4]arene (*AdC4A*) were studied. Using IR spectroscopy, it has been shown that in calixarene in dilute solution in CCl₄, there was no free hydroxyl absorption band. The hydroxyl group band was characterized by a very low frequency, which indicates a strong intramolecular hydrogen bond on the lower rim of the calixarene molecules. On the upper rim of the calixarene, the carboxyl groups form cyclic dimer or tetramer complexes via intermolecular hydrogen bonds. The cone conformation persists, but there is a mutual influence of the hydrogen bonds along the top and bottom rims of the calixarene molecule. The structure with dimeric hydrogen bonds between the carboxyl groups is 16.5 KJ/mol more preferable than the structure with tetrameric cyclic hydrogen bonds for *AdC4A*. The reactivity depends on the type of association on the upper rim, whether these are hydrogen-bonded dimers or cyclic tetrameric association.

Keywords Calixarenes · IR spectra · Hydrogen bonding · Normal vibrations · DFT

Introduction

One of the many applications of calixarenes is their use as multifunctional molecular receptors [1]. It has been found that the calixarenes carboxylated on the upper rim are molecular receptors for amines, metal ions, and aromatic hydrocarbons [2–4]. It is known that the conformational state of

calix[4]arenes with large *p*-tert-butyl substituents on the upper rim is a cone [1]. According to data from X-ray diffraction, IR, and NMR methods, there is a strong intramolecular hydrogen bond of the hydroxyl groups on the lower rim of the calix[4]arene macrocycle [5, 6].

It is also known that carboxylic acids form intermolecular dimeric hydrogen bonds of such a strength that even the sublimation of the sample takes place without breaking these intermolecular hydrogen bonds [7]. Earlier, we synthesized calix[4]arenes derivatives with hydroxyl groups on the lower rim and with adamantyl carboxylic moieties on the upper rim of the molecule [8]. The introduction of an adamantyl substituent must considerably increase the size of the intramolecular cavity and, by this means, modify the complexing properties of the calixarenes. Thus, adamantylcalixarenes can be useful new host molecules. The presence of the adamantane fragment exerts an essential influence on the extraction and ion transport properties of these molecules, and its functionalization is a promising tool for the design of synthetic receptors.

It is convenient to study the hydrogen bonds in calixarenes by IR spectroscopy [9–14]. In this work, the hydrogen bonds and the conformational state of the *p*-(3-carboxy-1-adamantyl)-calix[4]arene (*AdC4A*) having an enlarged hydrophobic cavity and H-bonds on the lower and upper rims were studied. It is interesting to know

Electronic supplementary material The online version of this article (<https://doi.org/10.1007/s00894-020-04441-1>) contains supplementary material, which is available to authorized users.

✉ V. L. Furer
furer@kgasu.ru

✉ V. I. Kovalenko
koval@ioipc.ru

¹ Kazan State Architect and Civil Engineering University, 1 Zelenaya, 420043 Kazan, Russia

² Kazan Department of Joint Supercomputer Center of Russian Academy of Sciences – Branch of Federal Scientific Center “Scientific Research Institute for System Analysis of the RAS”, 2/31 Lobachevski Str., 4200111 Kazan, Russia

³ Department of Chemistry, Moscow State University, 1-3 Lenin’s Hills, 119991 Moscow, Russia

⁴ A.E. Arbuzov Institute of Organic and Physical Chemistry, RAS, 8 Arbuzov Str, 420088 Kazan, Russia

how additional hydrogen bonds between carboxyl groups along the upper rim of the calixarenes affect the conformation of the molecule and the hydrogen bonding system of the hydroxyl groups on the lower rim. We have calculated the absorption curves of the dimer and tetramer complexes formed by carboxyl groups on the upper rim of the calixarene molecule. The strength of the hydrogen bond is expressed in terms of Wiberg bond indices. The reactivity of calixarene is explained in terms of calculated global descriptors. The calixarene studied is used to build new ionophores for biologically relevant ammonium guests [8]. Derivatives of adamantyl calixarenes are used for the extraction of radionuclides [8]. The data from this study may be useful in further applied studies of calixarenes.

Experimental

The *p*-(3-carboxy-1-adamantyl)-calix[4]arene (*AdC4A*) was synthesized using a one-step procedure from *p*-H-calix[4]arene and 3-carboxy-1-adamantol [8]. For comparison, the IR spectra of 3-carboxy-1-adamantol (*AdA*) were also studied (Fig. 1).

The melting and destruction temperatures of these compounds are quite high (350 °C and higher) [1]. To remove the residual water and the solvent from the calixarene cavity and to determine the changes in conformation and the hydrogen bonds, the IR spectra were studied at different temperatures. Gradually, the samples were heated to 180 °C.

The IR spectra of calixarene samples in KBr pellets were recorded on a Vector-22 Bruker FTIR-spectrophotometer in the range 4000–400 cm^{-1} with a resolution of 4 cm^{-1} . The solvent CCl_4 was passed through molecular sieves, 3 or 4 Å, before being practiced to remove the residual water. All solutions have been devised in a glove box to prevent moisture. The concentration of solutions, in CCl_4 , was $1 \cdot 10^{-4} \text{ mol} \cdot \text{l}^{-1}$, and the thickness of the cell was 2 cm.

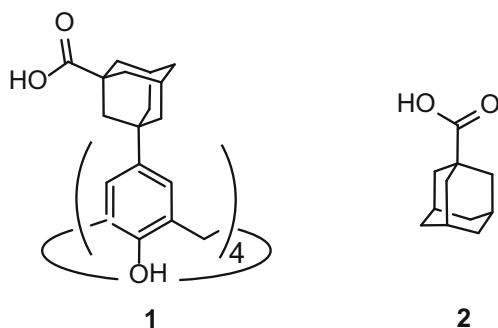


Fig. 1 Structure of *AdC4A* (1) and *AdA* (2)

Computational procedure

Of the four possible conformations of the calix[4]arenes cone, partial cone, 1,2- and 1,3-alternates, the cone conformation is the most energetically favorable [1]. Therefore, molecular models of *AdC4A* have been designed for cone conformation. At first, the geometry of the calix[4]arene in cone conformation was optimized. Next, adamantane substituents were attached to aromatic fragments of calix[4]arene in the para position. In the next step, carboxyl groups were attached to adamantane substituents. At the last stage, the carboxyl groups were oriented to obtain dimeric or tetrameric associates.

Optimization of the geometry and the computation of the IR spectra of *AdA* and *AdC4A* were carried out in the framework of the density functional theory using the Gaussian 09 software [15]. The exchange functional B3LYP and the basis set 6-31G(d,p) were used. The SHRINK software [16] was used to calculate the potential energy distribution. The assignment of the bands in the IR spectrum was taken out by relying on the potential energy distribution (PED). The calculations of the natural bonding orbital (NBO) [17] were carried out using Gaussian 09 software.

Results and discussion

In the IR spectra of the compounds *AdA* and *AdC4A* in the crystalline state and a diluted CCl_4 solution, there are no absorption bands of νOH without hydrogen bonding, nor about 3650 cm^{-1} for alcoholic hydroxyl groups nor about 3540 cm^{-1} for the acid hydroxyl (Figs. 2 and 3, Table 1). Therefore, we can conclude that in these molecules, all hydroxyl groups participate in the formation of intramolecular hydrogen bonds.

Besides, the alcoholic hydroxyl groups form a cyclic intramolecular hydrogen bond with a νOH frequency of 3152 cm^{-1} in the IR spectrum of a dilute solution in CCl_4 . The position of the νOH band of hydrogen-bonded hydroxyl acidic groups cannot, unfortunately, be determined because it is masked by the bands of the stretching vibrations of the CH groups (Fig. 3). Consequently, control of the mutual influence of the alcohol and acid hydrogen bonds in the molecules of the compounds studied is only possible for the νOH bands of hydroxyl groups and the $\nu\text{C}=\text{O}$ bands.

A comparison of the frequencies of the νOH hydroxyl groups in the IR spectra of the adamantyl (3226 cm^{-1}) and *p*-tert-butyl (3137 cm^{-1}) derivatives of calixarene in the crystalline state shows that the hydrogen bonds of carboxyl groups do not break the hydrogen bonds of hydroxyl alcohol groups. The conical conformation of these molecules persists.

The frequency of the $\nu\text{C}=\text{O}$ band depends on the hydrogen bonds of the carboxyl groups. In the IR spectrum of the *AdA* compound in the crystalline state, a broad complex band

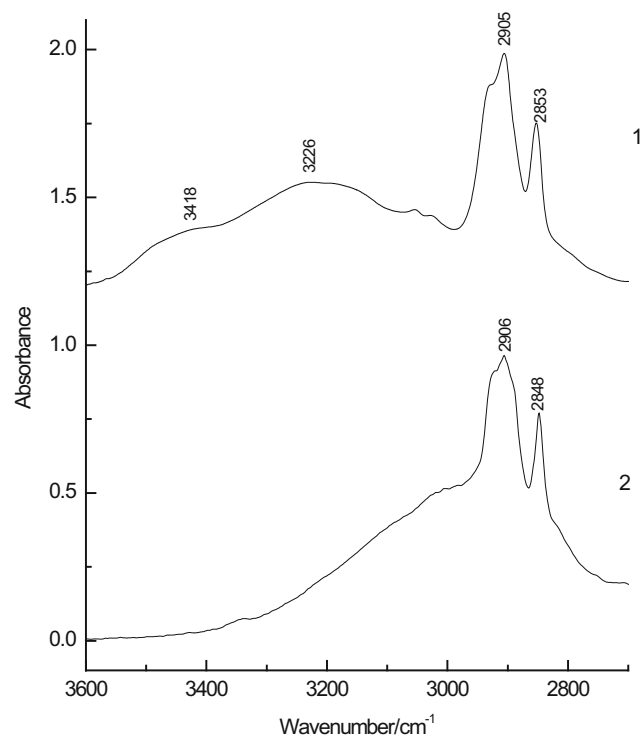


Fig. 2 Experimental IR spectra of crystalline *AdC4A* (1) and *AdA* (2) in the region 3600–2400 cm^{-1}

$\nu\text{C}=\text{O}$ at 1708 cm^{-1} is observed, which is characteristic of carboxyl groups forming an H-bond (Fig. 4). A doublet of bands at 1776 and 1697 cm^{-1} is observed in this region of

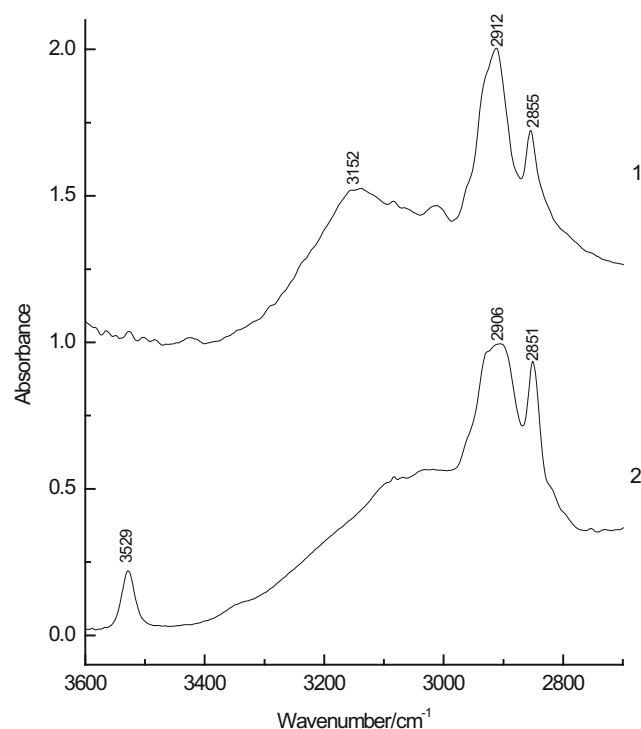


Fig. 3 Experimental IR spectra of *AdC4A* (1) and *AdA* (2) in dilute solutions in CCl_4 in the region 3600–2400 cm^{-1}

the IR spectra of the calixarene *AdC4A*. The first band refers to the vibrations of the free carboxyl groups, and the second corresponds to these groups involved in the formation of the H-bond.

The calixarene macrocycle spatially limits the formation of H-bonds between carboxyl groups. Under the influence of the hydrogen bonds on the upper rim of the calixarene molecules, the cooperation of the H-bonds of the hydroxyl groups decreases, and the frequency νOH increases.

The two variants of the formation of hydrogen bonds of carboxyl groups have been considered—H-bonded dimers and cyclic tetrameric chains. The formation of two H-bonded cyclic dimers, between adjacent carboxyl groups in the *AdC4A* molecule, was more energy-efficient than for cyclic tetramers; the energy difference was about 16.5 kJ/mol. The calculations showed that the molecule *AdC4A* with dimers of the carboxyl group and the molecule with hydrogen bonding tetrameric cycles have a cone conformation (Fig. 5, Supplementary information S1).

For a scheme with two H-bonded cyclic dimers between adjacent carboxyl groups, the average distance $r(\text{O}\cdots\text{O})$ is 2.65 \AA on the upper rim and 2.66 \AA on the lower rim. The distance $r(\text{O}\cdots\text{O})$ is 2.65 \AA for an external H-bond located at the periphery of the macrocycle, while the internal H-bond of the dimer, which is closer to the center of the macrocycle is at a distance $r(\text{O}\cdots\text{O})$ equal to 2.68 \AA . For a scheme with cooperative cyclic intramolecular hydrogen bonds between the four carboxyl groups, the average distance $r(\text{O}\cdots\text{O})$ is 2.67 \AA on the upper rim and 2.69 \AA on the lower rim (Fig. 5).

The structure of *AdC4A* with cooperative cyclic intramolecular H-bonds along the lower rim and a pair of carboxyl group H-bonds dimers on the upper rim is in good agreement with experimental IR data. At the same time, the presence of a shoulder at 1705 cm^{-1} ($\nu\text{C}=\text{O}$) leaves the possibility of the existence of a second variant of H-bond—the tetrameric chain on the upper rim. The formation of an H-bond along the upper rim of the molecule affects the intramolecular bonding of the lower rim. Thus, the intramolecular H-bonds are formed on the upper rim, but not intermolecular H-bonds.

The hydrogen bond strength can be described using the Wiberg bond indices [18]. For the molecule *AdC4A*, the average order of the H-bonds of the cycle on the lower rim is 0.097, and in the dimer associations of the carboxyl groups on the upper rim, it is 0.089. The corresponding values are 0.086 and 0.085 for the cycles on the lower and upper rims of the cyclic arrangement of the carboxyl hydrogen bonding network. Thus, the H-bonds on the upper and lower rims of the calixarene molecules influence each other.

The torsional angles $\varphi(\text{C}26\text{--C}30\text{--C}2\text{--C}13)$ and $\chi(\text{C}30\text{--C}2\text{--C}13\text{--C}17)$ determine the conformation of the calixarenes [19]. The mean absolute values of the torsion angles of the molecule *AdC4A* for the dimeric associations of carboxyl groups are equal to 90.8 and 90.9° , and for the cyclic

Table 1 Experimental frequencies of ν_{OH} (cm^{-1}) of crystals and dilute solutions of AdC4A in CCl_4

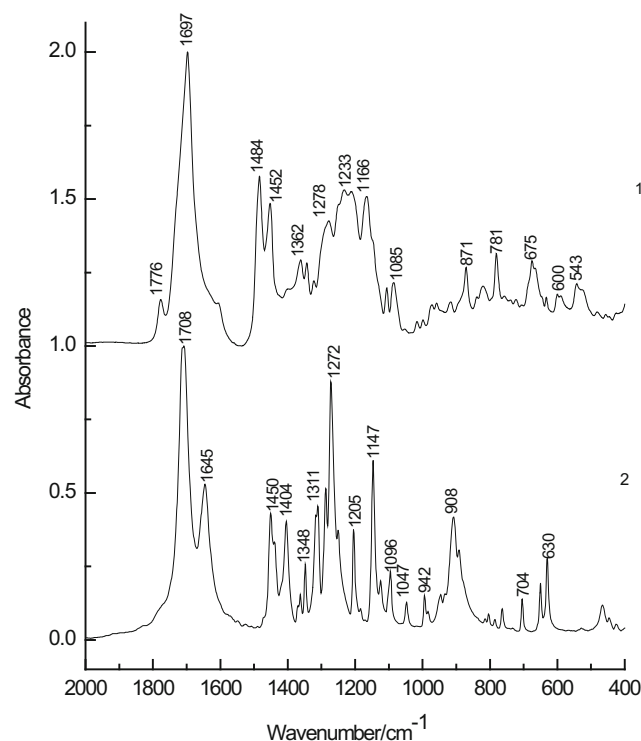
Original crystals, T_{room}	Heated crystals, $T = 180\text{ }^{\circ}\text{C}$	Cooled crystals, T_{room}	Solution in CCl_4
3226, 3418	3251, 3534 sh	3228	3152

tetrameric H-bonds, they are 86.5 and 89.7° (Supplementary information S2). Thus, the association of carboxyl groups on the upper rim of the calixarene AdC4A affects the orientation of the aromatic fragments. The other geometric parameters of the AdC4A molecule change only slightly (Supplementary information S1).

First, we calculated the IR spectra of the model compound AdA, then the IR spectra of the calixarene AdC4A with dimer and tetrameric associations on the upper rim (Table 2, Supplementary information S3–S6). Such a calculation allows the assignment of bands in the experimental IR spectrum of the calixarene AdC4A.

The vibrational bands of the stretching of the CH bonds are seen in the region of $2800\text{--}3000\text{ cm}^{-1}$ of the experimental IR spectra of AdA and AdC4A (Fig. 2). The IR spectra of the two compounds in this region are very similar and contain bands at 2906 and 2848 cm^{-1} and the shoulder at 2930 cm^{-1} due to the CH stretching vibrations.

The bands at 1450 , 1439 , and 1404 cm^{-1} in the experimental IR spectrum of AdA include the deformation vibrations of the methylene groups (Fig. 4, Table 3). The band at 1484 cm^{-1} in the IR spectrum of AdC4A is caused by the bending vibrations of the methylene groups of the macrocycle. The band at

**Fig. 4** Experimental IR spectra of crystalline AdC4A (1) and AdA (2) in the region $1800\text{--}400\text{ cm}^{-1}$

1452 cm^{-1} is assigned to the corresponding vibrations of the adamantyl substituent.

The IR spectrum of AdA shows bands at 1370 , 1363 , 1348 , 1316 , and 1311 cm^{-1} attributed to the deformation of the CH bond and wagging vibrations of the methylene groups. These

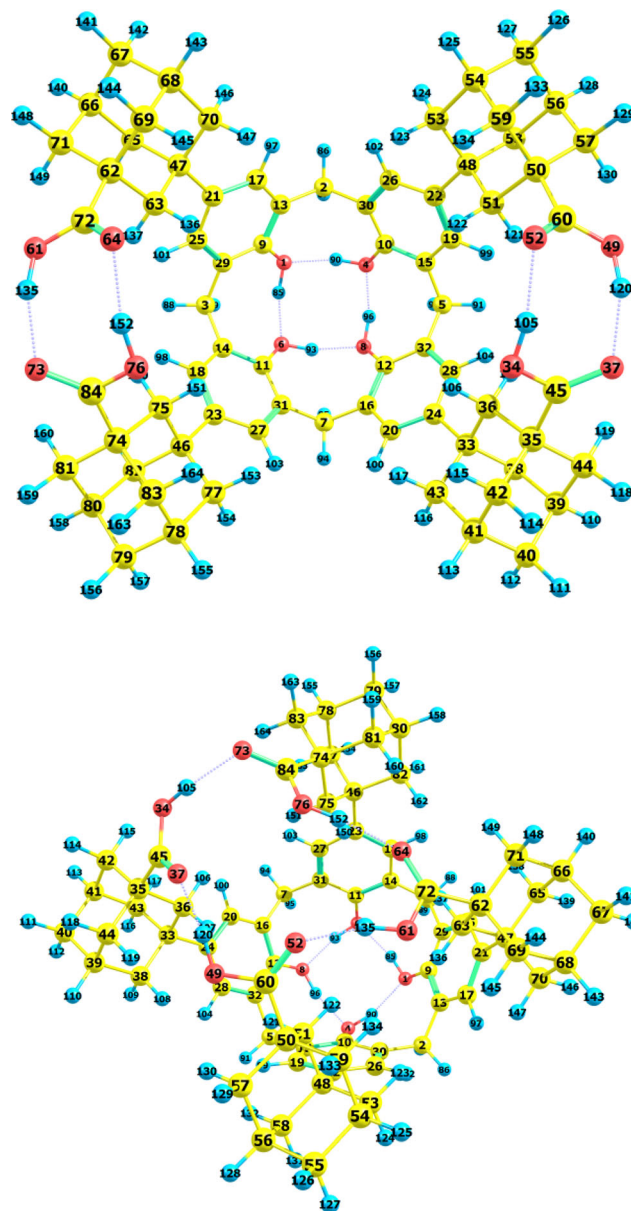
**Fig. 5** Optimized geometry and atom numbering for AdC4A in the conformation cone with a cyclic system of hydrogen bonds along the lower rim and dimers (1) and cyclic hydrogen bonds along the upper rim (2). Yellow, blue and red colors correspond to carbon, hydrogen, and oxygen atoms

Table 2 Experimental and corresponding calculated frequencies (cm^{-1}), intensity *I* (km/mol) of bands in the IR spectra of AdA in the region 1800–400 cm^{-1}

Exp.	Calculated		Assignment by PED in internal coordinates
ν	ν	<i>I</i>	
1777	1766	256.2	83 $\nu(\text{C}=\text{O})$, 5 $\nu(\text{CC})$, 3 $\nu(\text{CO})$
1697			
1591			
1562			
	1475	0.8	69 $\chi(\text{CC})$, 20 $\delta(\text{HCH})$, 8 $\delta(\text{CCH})$
1456	1455	11.5	60 $\chi(\text{CC})$, 22 $\delta(\text{HCH})$, 10 $\delta(\text{CCH})$
	1454	6.8	60 $\chi(\text{CC})$, 20 $\delta(\text{HCH})$, 11 $\delta(\text{CCH})$
	1450	7.3	72 $\chi(\text{CC})$, 22 $\delta(\text{HCH})$, 10 $\delta(\text{CCH})$
	1440	0.5	64 $\chi(\text{CC})$, 21 $\delta(\text{HCH})$, 12 $\delta(\text{CCH})$
	1437	0.4	71 $\chi(\text{CC})$, 20 $\delta(\text{HCH})$, 10 $\delta(\text{CCH})$
1396			
1360	1355	1.2	33 $\delta(\text{CCH})$, 29 $\chi(\text{CC})$, 24 $\nu(\text{CC})$
	1352	0.3	35 $\delta(\text{CCH})$, 29 $\chi(\text{CC})$, 22 $\nu(\text{CC})$
1342	1350	1.8	43 $\delta(\text{CCH})$, 31 $\chi(\text{CC})$, 14 $\nu(\text{CC})$
	1335	0.0	45 $\delta(\text{CCH})$, 27 $\chi(\text{CC})$, 16 $\nu(\text{CC})$
	1335	0.3	41 $\delta(\text{CCH})$, 27 $\chi(\text{CC})$, 17 $\nu(\text{CC})$
1321	1325	28.1	26 $\nu(\text{CC})$, 17 $\nu(\text{CO})$, 6 $\delta(\text{OCO})$
	1307	0.0	51 $\delta(\text{CCH})$, 45 $\chi(\text{CC})$
	1302	0.1	37 $\delta(\text{CCH})$, 32 $\chi(\text{CC})$, 20 $\nu(\text{CC})$
	1301	0.9	36 $\delta(\text{CCH})$, 27 $\chi(\text{CC})$, 18 $\nu(\text{CC})$
	1293	21.2	34 $\delta(\text{CCH})$, 27 $\chi(\text{CC})$, 25 $\nu(\text{CC})$
1276	1276	1.4	39 $\nu(\text{CC})$, 35 $\delta(\text{CCH})$, 11 $\chi(\text{CC})$
	1273	0.1	41 $\nu(\text{CC})$, 38 $\delta(\text{CCH})$, 7 $\chi(\text{CC})$
	1271	0.0	39 $\nu(\text{CC})$, 36 $\delta(\text{CCH})$, 12 $\chi(\text{CC})$
	1250	4.2	42 $\delta(\text{CCH})$, 28 $\chi(\text{CC})$, 20 $\nu(\text{CC})$
	1238	0.0	38 $\delta(\text{CCH})$, 33 $\chi(\text{CC})$, 17 $\nu(\text{CC})$
1222			
1210			
1186	1176	32.6	43 $\delta(\text{CCH})$, 25 $\chi(\text{CC})$, 10 $\nu(\text{CC})$
1170	1164	0.0	41 $\chi(\text{CC})$, 31 $\delta(\text{CCH})$, 12 $\nu(\text{CC})$
1150	1139	155.9	34 $\delta(\text{COH})$, 18 $\nu(\text{CO})$, 7 $\delta(\text{CCH})$
1107	1097	0.0	50 $\delta(\text{CCH})$, 44 $\chi(\text{CC})$
	1094	0.0	49 $\delta(\text{CCH})$, 43 $\chi(\text{CC})$
	1087	0.1	43 $\chi(\text{CC})$, 38 $\delta(\text{CCH})$, 15 $\nu(\text{CC})$
	1083	1.8	41 $\chi(\text{CC})$, 37 $\delta(\text{CCH})$, 11 $\nu(\text{CC})$
1081	1081	21.5	40 $\chi(\text{CC})$, 37 $\delta(\text{CCH})$, 11 $\nu(\text{CC})$
1052	1054	61.4	42 $\nu(\text{CO})$, 10 $\delta(\text{CCC})$, 7 $\nu(\text{CC})$
1031	1020	3.6	53 $\nu(\text{CC})$, 13 $\delta(\text{CCH})$, 12 $\nu(\text{CO})$
	1014	0.0	64 $\nu(\text{CC})$, 14 $\delta(\text{CCH})$, 3 $\chi(\text{CC})$
999	1010	0.4	63 $\nu(\text{CC})$, 15 $\delta(\text{CCH})$, 8 $\chi(\text{CC})$
973	957	0.8	36 $\chi(\text{CC})$, 35 $\nu(\text{CC})$, 18 $\delta(\text{CCH})$
958	955	4.6	33 $\chi(\text{CC})$, 28 $\nu(\text{CC})$, 17 $\delta(\text{CCH})$
946	954	3.3	36 $\chi(\text{CC})$, 34 $\nu(\text{CC})$, 13 $\delta(\text{CCH})$
923	914	0.0	64 $\nu(\text{CC})$, 12 $\delta(\text{CCC})$, 8 $\chi(\text{CC})$
892	910	4.2	65 $\nu(\text{CC})$, 7 $\delta(\text{CCC})$, 6 $\chi(\text{CC})$
874	871	0.0	40 $\nu(\text{CC})$, 32 $\chi(\text{CC})$, 8 $\delta(\text{CCH})$

Table 2 (continued)

Exp.	Calculated		Assignment by PED in internal coordinates
	869	0.0	64 $\chi(\text{CC})$, 21 $\delta(\text{CCH})$, 6 $\nu(\text{CC})$
	863	0.1	58 $\chi(\text{CC})$, 18 $\nu(\text{CC})$, 15 $\delta(\text{CCH})$
832	862	1.4	70 $\chi(\text{CC})$, 22 $\delta(\text{CCH})$, 10 $\nu(\text{CC})$
795	799	1.4	62 $\nu(\text{CC})$, 21 $\chi(\text{CC})$, 4 $\delta(\text{CCC})$
787	788	1.6	68 $\nu(\text{CC})$, 15 $\chi(\text{CC})$
740	747	0.1	86 $\nu(\text{CC})$
	729	30.2	34 $\nu(\text{CC})$, 30 $\chi(\text{CO})$, 27 $\chi(\text{CC})$
674	689	7.9	60 $\nu(\text{CC})$, 10 $\nu(\text{CO})$, 6 $\delta(\text{CCC})$
667	632	0.9	41 $\chi(\text{CC})$, 23 $\delta(\text{CCC})$, 15 $\nu(\text{CC})$
633	632	0.1	47 $\chi(\text{CC})$, 23 $\delta(\text{CCC})$, 14 $\nu(\text{CC})$
627	624	44.5	34 $\delta(\text{OCO})$, 14 $\delta(\text{OCC})$, 13 $\delta(\text{COH})$
547	589	75.3	92 $\chi(\text{CO})$
535			
486	478	4.1	40 $\delta(\text{OCC})$, 20 $\chi(\text{CC})$, 11 $\nu(\text{CC})$
469	456	6.1	83 $\chi(\text{CC})$, 5 $\delta(\text{CCC})$, 4 $\nu(\text{CC})$
442	426	0.0	84 $\chi(\text{CC})$, 8 $\delta(\text{CCC})$
424	419	0.2	85 $\chi(\text{CC})$, 8 $\delta(\text{CCC})$, 3 $\delta(\text{OCC})$
411	392	0.1	61 $\nu(\text{CC})$, 34 $\delta(\text{CCC})$

oscillations appear as bands at 1362, 1343, and 1323 cm^{-1} in the IR spectrum of *AdC4A* (Fig. 4).

The bands at 1287, 1272, 1251, and 1205 cm^{-1} in the IR spectrum of *AdA* are caused by stretching vibrations of the CC and CO bonds, as well as deformation vibrations of the CH bonds and the twist of the methylene groups. Similar bands are observed at 1289, 1278, 1250, 1233, and 1211 cm^{-1} in the IR spectrum of *AdC4A*.

The bands 1184, 1147, 1125, and 1101 cm^{-1} of the *AdA* IR spectrum are attributed to the twisting vibrations of the methylene groups and the deformation vibrations of the CH bonds. The corresponding vibrations cause bands at 1166, 1147, and 1105 cm^{-1} in the IR spectrum of *AdC4A*.

The bands at 1096 and 1047 cm^{-1} in the IR spectrum of *AdA* are due to the CC stretching vibrations and the twisting vibrations of the methylene groups. These vibrations appear as bands at 1086, 1053, and 1016 cm^{-1} in the IR spectrum of *AdC4A*.

The bands at 994, 984, 952, 946, 933, and 908 cm^{-1} in the IR spectrum of *AdA* have been attributed to the stretching vibrations of the CC bonds, to the rocking vibrations of the methylene groups and the bending vibrations of the CCC angles. These vibrations lead to bands at 999, 972, 956, and 916 cm^{-1} in the IR spectrum of *AdC4A*.

The stretching vibrations of the CC bonds and the rocking vibrations of the methylene groups induce the appearance of bands at 892, 880, 814, and 804 cm^{-1} in the IR spectrum of *AdA*. Similar vibrations cause the bands at 894, 870, 839, and 820 cm^{-1} in the *AdC4A* IR spectrum.

Table 3 Global reactivity descriptors of *AdA* and *AdC4A*

System	Ionization energy, eV	Electron affinity, eV	Chemical potential, eV	Softness, eV	Electrophilicity index, eV	Dipole moment, D
<i>AdA</i>	9.120	−2.678	−3.221	0.085	0.879	1.705
<i>AdC4A</i> , dimer	6.822	−0.452	−3.185	0.137	1.395	1.515
<i>AdC4A</i> , tetramer	6.821	−0.423	−3.199	0.138	1.413	3.180

The stretching vibrations of the CC bonds determine the bands at 785, 764, 744, 733, and 704 cm^{-1} in the IR spectrum of *AdA*. The corresponding vibrations appear as bands at 781, 758, 739, 723, and 706 cm^{-1} in the IR spectrum of *AdC4A*.

The bending vibrations of the CCC angles cause bands at 650 and 630 cm^{-1} in the IR spectrum of *AdA*. The bands at 686, 675, 666, 646, 633, and 600 cm^{-1} in the IR spectrum of *AdC4A* have been identified as deformation vibrations of skeletal angles.

Bands at 529, 466, 447, and 426 cm^{-1} of the *AdA* IR spectrum have been allocated to the deformation vibrations of the molecule skeleton and the torsional vibrations around the CC bonds. The bands at 590, 543, 525, 482, 456, 446, 426, and 412 cm^{-1} in the IR spectrum of the *AdC4A* are also caused by deformation and torsion vibrations of the macrocycle and the molecular skeleton.

It is interesting to determine the differences in the IR spectra of the calixarene *AdC4A* for the dimer and tetramer associations of the carboxyl groups on the upper rim of the molecule (Fig. 6). A comparison of the theoretical IR spectra of *AdC4A* molecules shows the characteristic bands as follows: 1457, 1252, 1203, 1091, and 720 cm^{-1} (dimer); 1235, 1123, 1087, and 935 cm^{-1} (tetramer) (Fig. 6, Supplementary information S6). Since the difference in energy between the two types of associates is not very large, both forms can exist in the crystalline state, and the distinct bands in the IR spectra allow them to be identified.

In this article, we have also attempted to describe the reactivity of calixarene using global descriptors (Table 3). Ionization energy and electron affinity decrease in *AdC4A* compared to *AdA*. The chemical potential, calculated as $\mu \approx -(IE + EA)/2$, describes the ability of electrons to leave the system [20]. The value of the chemical potential is comparable in the molecules *AdC4A* and *AdA*.

The chemical hardness $\eta \approx (IE - EA)$ defines the resistance to modification of the electronic distribution [20]. The inverse hardness is called softness $S = 1/2\eta$ [20]. The softness of the calixarene molecules increases with the transition to *AdC4A* from *AdA*. The global electrophilic index $\omega = \mu^2/2\eta$ determines the reduction in energy caused by the maximum transfer of electrons from the donor to the acceptor [20]. This index and dipole moment are maximal for *AdC4A* tetramer. The reactivity of the calixarenes strongly depends on the type of association on the upper rim.

Summary

For *AdC4A* molecules in diluted solutions in CCl_4 , an intramolecular hydrogen bond between adjacent carboxyl groups occurs along the upper rim. These are hydrogen-bonded dimers of neighboring carboxyl groups. The structure of the molecules is determined by the mutual influence of two hydrogen-bonded macrocycles between the carboxyl (upper rim) and hydroxyl (lower rim) groups. The formation of an intramolecular hydrogen bond between the carboxyl groups on the upper rim of the calixarene molecules only slightly weakens the cooperative cyclic intramolecular hydrogen bond on the lower rim of the macrocycle.

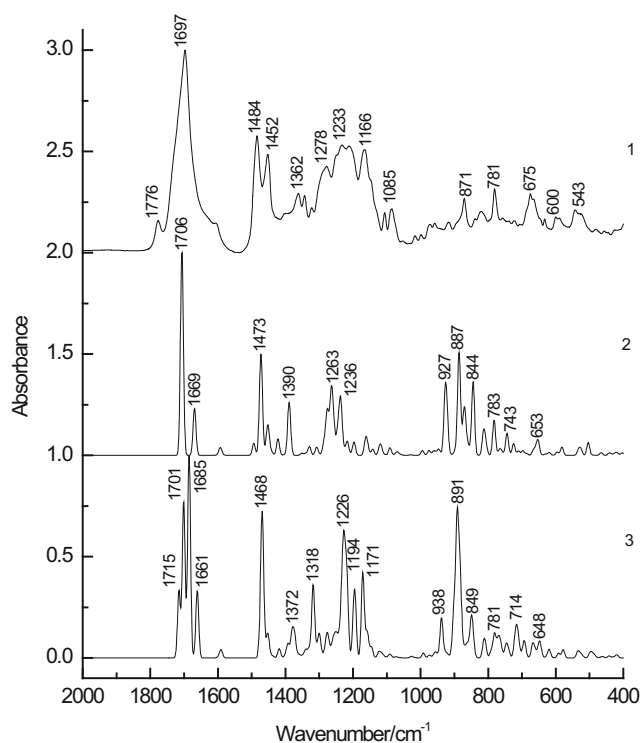


Fig. 6 Experimental (1) and theoretical IR spectra of *AdC4A* in the conformation cone with a cyclic system of hydrogen bonds along the lower rim and dimers (2) and cyclic hydrogen bonds (3) along the upper rim in the region 1800–400 cm^{-1}

Acknowledgments The authors are grateful to the Assigned Spectral-Analytical Center of FRC Kazan Scientific Center of RAS for technical assistance in research.

Funding information Contributions to research were funded by the state assignment to: Federal Scientific Center “Scientific Research Institute for System Analysis of the RAS” (CDV) and A.E. Arbuzov Institute of Organic and Physical Chemistry RAS (V.I.K.).

References

- Vicens J, Harrowfield J, Baklouti L (eds) (2007) Calixarenes in the nanoworld. Springer, Dordrecht
- Neri P., Sessler J., Wang M.-X.(Ed.).: Calixarenes and beyond. Springer International Publishing, Switzerland, (2016)
- Pellet-Rostaing S, Chitry F, Nicod L, Lemaire M (2001) Synthesis and complexation properties of 1,3-alternate calix[4]arene-bis(crown-6)derivatives. J Chem Soc Perkin Trans 2:1426–1432
- Gutsche CD, Iftikhar A (1988) Calixarenes. 23. The complexation and catalytic properties of water soluble calixarene. Tetrahedron 44: 4689–4694
- Konig B, Fonseca MH (2000) Heteroatom-bridged calixarenes. Eur J Inorg Chem 2000:2303–2310
- Opaprakasit P, Scaroni A, Painter P (2001) Intramolecular hydrogen bonding and calixarene-like structures in p-cresol/formaldehyde resins. J Mol Struct 570:25–35
- Bellamy L (1975) The infra-red spectra of complex molecules. Springer
- Shokova EA, Motomaya AE, Shestakova AK, Kovalev VV (2004) p-(3-Carboxy- and 3-carboxymethyl-1-1adamantyl)calix[4]arenes: synthesis and arming with amino acid units. Tetrahedron Lett 45: 6465–6469
- Katsyuba SA, Kovalenko VI, Chernova AV, Vandyukova EE, Zverev VV, Shagidullin RR, Antipin IS, Solovieva SE, Stoikov I, Konovalov AI (2005) Vibrational spectra, co-operative intramolecular hydrogen bonding and conformations of calix[4]arene and thiacalix[4]arene molecules and their *para-tert-butyl* derivatives. Org Biomol Chem 3:2558–2565
- Furer VL, Borisoglebskaya EI, Kovalenko VI (2005) Band intensity in the IR spectra and conformations of calix[4]arene and thiacalix[4]arene. Spectrochim Acta 61:355–359
- Furer VL, Borisoglebskaya EI, Zverev VV, Kovalenko VI (2005) The hydrogen bonding and conformations of *p-tert-butylcalix[4]arene* as studied by IR spectroscopy and by DFT calculations. Spectrochim Acta 62:483–493
- Furer VL, Borisoglebskaya EI, Zverev VV, Kovalenko VI (2006) DFT and IR spectroscopic analysis of *p-tert-butylthiacalix[4]arene*. Spectrochim Acta 63:207–212
- Furer VL, Potapova LI, Kovalenko VI (2017) DFT study of hydrogen bonding and IR spectra of calix[6]arene. J Mol Struct 1128: 439–447
- Furer VL, Potapova LI, Vatsouro IM, Kovalev VV, Shokova EA, Kovalenko VI (2019) Study of conformation and hydrogen bonds in the *p*-1-adamantylcalix[8]arene and IR spectroscopy and DFT. J Incl Phenom 95:63–71
- Frisch MJ, Trucks GW, Schlegel HB, Scuseria GE, Robb MA, Cheeseman JR, Scalmani G, Barone V, Mennucci B, Petersson GA, Nakatsuji H, Caricato M, Li X, Hratchian HP, Izmaylov AF, Bloino J, Zheng G, Sonnenberg JL, Hada M, Ehara M, Toyota K, Fukuda R, Hasegawa J, Ishida M, Nakajima T, Honda Y, Kitao O, Nakai H, Vreven T, Montgomery JA, Peralta JE, Ogliaro F, Bearpark M, Heyd JJ, Brothers E, Kudin KN, Staroverov VN, Keith T, Kobayashi R, Normand J, Raghavachari K, Rendell A, Burant JC, Iyengar SS, Tomasi J, Cossi M, Rega N, Millam JM, Klene M, Knox JE, Cross JB, Bakken V, Adamo C, Jaramillo J, Gomperts R, Stratmann RE, Yazyev O, Austin AJ, Cammi R, Pomelli C, Ochterski JW, Martin RL, Morokuma K, Zakrzewski VG, Voth GA, Salvador P, Dannenberg JJ, Dapprich S, Daniels AD, Farkas O, Foresman JB, Ortiz JV, Cioslowski J, Fox DJ (eds) (2010) Gaussian 09 Revision C.01. Gaussian Inc., Wallingford
- Sipachev VA (1985) Calculation of shrinkage corrections in harmonic approximation. J Mol Struct (THEOCHEM) 121:143–151
- Glendening ED, Landis CR, Weinhold F (2012) Natural bond orbital methods. Comput Mol Sci 2:1–42
- Wiberg KA (1968) Application of the pople-santry-segal CNDO method to the cyclopropylcarbinyl and cyclobutyl cation and to bicyclobutane. Tetrahedron. 24:1083–1096
- Ugozzoli F, Andretti GD (1992) Symbolic representation of the molecular conformation of calixarenes. J Incl Phenom 13:337–348
- Parr RG, Pearson RG (1983) Absolute hardness: companion parameter to absolute electronegativity. J Am Chem Soc 105:7512–7516

Publisher's note Springer Nature remains neutral with regard to jurisdictional claims in published maps and institutional affiliations.